SHORT COMMUNICATION

Biodegradable deep-eutectic mixtures as electrolytes for the electrochemical synthesis of conducting polymers

Paula M. V. Fernandes · José M. Campiña ·
Nuno M. Pereira · Carlos M. Pereira ·
Fernando Silva

Abstract The use of inexpensive and biodegradable deep-eutectic ionic mixtures as solvents for the electrochemical synthesis of conducting polymers could potentially improve the sustainability of these processes and reduce their economic cost. Such an unexplored approach was investigated in this communication by growing a model polymer such as polyaniline from a 1:2 mixture of choline chloride and 1,2-ethanediol (the so-called Propeline) using potentiodynamic and potentiostatic electrochemical procedures. Beyond a preparation method, cyclic voltammetry was also used to characterize the growth of the polymers. The morphology of the films, and their optical properties, were assessed ex-situ by means of scanning electron microscopy and spectroscopic measurements in the UV–vis. The polyanilines thus prepared exhibited nanoparticulated morphology and high reversibility to doping/dedoping which evidences fast charge transport across the films. Excellent conductivities higher than 50 S cm^{-1} were found under this approach.

P. M. V. Fernandes · J. M. Campiña (✉) ·
N. M. Pereira · C. M. Pereira · F. Silva
Centro de Investigação em Química (CIQ-L4), Departamento de Química e Bioquímica, Faculdade de Ciências, Universidade do Porto, Rua do Campo Alegre 687, 4169-007 Porto, Portugal
e-mail: jpina@fc.up.pt

P. M. V. Fernandes
e-mail: paula.vale.fernandes@gmail.com

N. M. Pereira
e-mail: nuno_pereira@oniduo.pt

C. M. Pereira
e-mail: cmpereir@fc.up.pt

F. Silva
e-mail: afssilva@fc.up.pt

1 Introduction

The great chemical stability, high ionic conductivity, good solubility, very low vapor pressure, and non-flammability of room temperature ionic liquids (RTILs) have attracted immense attention from many areas of chemistry and industry [1–3]. As their recycling seems also feasible [4], RTILs have been pointed as "green" alternatives to substitute traditional solvents in organic synthesis [5], catalysis [6], electroplating [7], and so forth. The deep-eutectic solvents (DES) are a special type of ionic liquids which can be considered a low cost alternative to RTILs [8]. DES are typically prepared by mixing salts of ammonium, phosphonium, and other analogs (with choline chloride being part of the better studied systems) with a series of hydrogen bond donors (HBDs; acids, amines, alcohols, and so forth) to form an eutectic which melting point is lower than those for their individual components [9].

The applications of these liquids as electrolytes in electrochemical processes involve, to date, studies on metal deposition (and their dissolution in electropolishing treatments) [10] and their use in the dye-sensitized solar cell (DSSC) [11]. Other applications involve biologic processes such as the hydrolase catalyzed biotransformation [12] or the extraction of glycerol from biodiesel [13]. However, to the best of our knowledge, the potential of deep-eutectic mixtures as solvents in organic synthesis has not been adequately explored and the electropolymerization of organic semiconductors from these mixtures has not been approached before.

In this respect, polyaniline (PANI) is one of the most important organic semiconductors to be tested as a model due to its good environmental stability, high electrical conductivity, easy of synthesis, and a quite reversible doping/dedoping chemistry. These properties have led to their widespread utilization in devices for energy conversion and storage (including supercapacitors, batteries, and anodes for fuel cells) [14, 15], sensors and biosensors [16], electrocatalysis [17], gas separation [18], and electrochromic displays [19].

In recent years, organic semiconductors prepared from RTILs have exhibited interesting properties in terms of stability, morphology, and surface area. Judging from the similarities between RTILs and DES, it is hypothesized that replacing the first ones by DES will bring polymers with electrochemical and optical performances very similar to those produce from RTILs, but at a much lower economic and environmental cost. In this context, choline is a naturally occurring biocompatible compound which is not hazardous if it is released back to nature (pure or in the form of a deep-eutectic mixture) following rapid biodegradation [13, 20]. 1,2-propanediol is also a readily biodegradable substance that can be used as HBD [21]. Since choline chloride and 1,2-propanediol are inexpensive, the industrial processes using their mixtures will also be more economically viable. With the purpose of studying the feasibility of electropolymerization processes in them, the electrosynthesis of the well-known PANI has been attempted in an acidic mixture of choline chloride and 1,2-propanediol, the so-called Propeline [22].

2 Preparation of PANI

Choline chloride (ChCl; Sigma–Aldrich, 98.0 %) and 1,2-propanediol (Sigma–Aldrich) were mixed in a 1:2 ratio and continuously stirred at 60 °C, in a thermostated three electrode water jacketed cell, until an homogeneous and colorless liquid was formed. The water content was estimated to be between 300 and 400 ppm by means of the Karl Fisher titration method. Then, aniline (Sigma–Aldrich, 99.5 %) and sulfuric acid (Sigma–Aldrich, 98.5 %) were added to the mixture to final concentrations of 0.7 and 1 M, respectively.

A Voltalab PGZ301 (Radiometer) potentiostat (controlled through the software Voltammaster 4) was used for the electrochemical measurements. Pt and Ag wires were used as counter and pseudo-reference electrodes, respectively. The working electrode was a GCE (Metrohm, 0.0314 cm^2 area) polished with polycrystalline diamond suspensions (1 and 3 μm) and sonicated for 15 min in ultrapure water (18 MΩ cm) before its use. DES solutions were de-aireated with N$_2$ (N45 Air Liquid) for 15 min before each experiment. PANI films were, then, grown using the potentiodynamic cyclic voltammetry (CV) and a potentiostatic chronoprocedure.

3 Results and discussion

3.1 Electrochemistry

Figure 1a illustrates the potentiodynamic growth of PANI from the Propeline electrolytic solution described above (CV-PANI-Prop). A selection of the first 40 CV-scans applied between −0.2 and +1.4 V (vs Ag wire), at 100 mV s^{-1} and 60 °C, is presented in the figure (just the odd ones are shown). The first recorded scan (see figure inset) presented a broad anodic peak around the upper limit which is ascribed to the oxidation of aniline monomers. Such a step initiates the polymerization process and, then, a
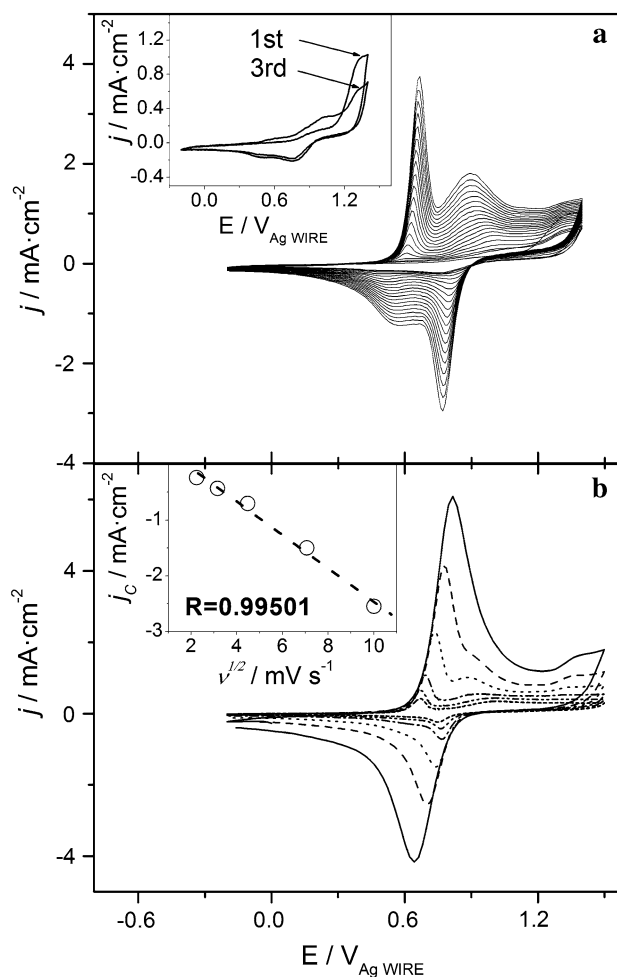

Fig. 1 a CVs obtained for GCE in 0.7 M aniline + 1 M H$_2$SO$_4$ solutions in Propeline at 60 °C during the electrosynthesis of PANI with 40 scans (just the odd ones are shown). The *inset* presents details on the evolution of the first 3 scans. The scan rate was 100 mV s^{-1}. **b** CVs registered for CV-PANI-Prop films prepared with the same number of CV-scans applied in **a**, and in the same medium, at different scan rates: 200, 100, 50, 20, 10, and 5 mV s^{-1}. The *inset* displays the current density at the main cathodic peak for each case (j_C, *empty circles*) versus the square root of the scan rate ($v^{1/2}$). The *dashed line* represents the linear fitting of the experimental data

film of PANI is subsequently grown, as deduced from the subsequent decrease of this peak scan upon scan. The continuous reduction in the amount of sites available for monomer oxidation on the surface of GCE, due to the physical deposition of the electrosynthesized polymer, may likely explain the evolution of this peak. Importantly, this behavior reflects as well that CV-PANI-Prop does not follow an autocatalytic mechanism, agreeing with that observed in aqueous media [23, 24].

Simultaneous with the decrease in this peak, a couple of redox pairs developed with increasing the number of scans. The shape of the corresponding CVs agreed quite well with those previously reported for the electrochemical doping/dedoping of films prepared from aqueous solutions (CV-PANI-H_2O), also characterized by a couple of quase-reversible redox waves [25–28]. The greater was the number of collected cycles the higher were the peak currents recorded. This behavior also suggests that the load of polymer deposited onto the GCE surface (and subsequently following doping/dedoping upon potential change) continuously grew along the time of the experiment. It is well-known that PANI films prepared in aqueous acidic media (PANI-H_2O) are formed by domains of repeated benzenoid rings (Leuco-emeraldine Base, LB, a fully reduced, yellow, and electrically insulating state), alternated benzenoid and quinoid rings (Emeraldine Salt, ES; proton-doped, green, and conducting intermediate state), and repeated quinoid rings (Pernigraniline Base, PB; a fully oxidized, violet, and also insulating state) [25, 28, 29]. The transition between each of these states in acidic aqueous electrolyte involves the coupled transfer of 2 electrons and 2 protons, and can be induced electrochemically by imposing a certain electrode potential.

By comparison with the well-known CV-PANI-H_2O system, we can ascribe the first pair of peaks (placed at +0.67/+0.58 V in the CVs of Fig. 1a) to the oxidative transition from LB to ES and its posterior reduction in the negative-going potential excursion. Analogously, the pair at +0.89/+0.77 V may correspond to the further oxidation of ES to PB and its backwards reaction [25, 28]. Under certain conditions, CV-PANI-H_2O can present, located among them, a third pair of peaks which has been lately attributed to the redox activity of p-benzoquinone/hydroquinone (BQ/HQ) side species formed upon overoxidation of PB [28]. Figure 1a demonstrates that despite the high upper potential used in these experiments, CV-PANI-Prop can be grown upon a high number of scans without the presence of these peaks or without observation of overall peak decay, which might be taken as evidence supporting the good stability of the films prepared under these limited experimental conditions (films were prepared under identical conditions with more than 50 scans for conductivity measurements, as it is discussed below). Thus, although more stable PANI could be grown (with a higher number of

scans) using lower potentials, such a high potential was initially chosen to guarantee the achievement of reasonable polymerization rates in this solvent [30]. Interestingly, and in contrast to that seen for dense matrices of CV-PANI-H_2O, the short peak-to-peak potential differences measured in this case ($\Delta E_P \approx 100$ mV for both pairs) are a first indication of the high degree of reversibility of redox processes for CV-PANI-Prop.

The effect of scan rate, v, on the characteristics of CV-PANI-Prop was also investigated. Panel 1b compares the CVs recorded at several scan rates ranging between 5 and 200 mV s^{-1} for the film prepared in panel 1a. Remarkably, the redox waves described herein were shown to progressively merge into one single pair upon increasing the scan rate. This is likely due to the difficulties to resolve the two charge transfer processes involved in the doping/dedoping of the polymer within the time domain given for the experiments at high scanning rates. The inset of Fig. 1b correlates the current density at the main cathodic peak (j_C) with $v^{1/2}$. The data fitted quite well to a straight line ($R^2 = 0.995$). Linear j_C versus $v^{1/2}$ plots are usually taken as confirmation that redox processes are controlled by the slow diffusion of solution species toward the electrode. Hence, the diffusion of anions and water into/out of the polymer film during its potential-assisted doping/dedoping (which is necessary to balance the changes induced in polymer charge), seems to control the kinetics of the process. This behavior has been observed, and confirmed by means of in situ EQCM measurements, for other polymers synthesized electrochemically [31]. The high viscosity of Propeline at room temperature (89 cP) [7] could contribute to the slow diffusion of solution species [32]. However, this handicap has been balanced in these experiments by keeping the electrolyte at a constant temperature of 60 °C. The conclusion is that other factors may also contribute to this behavior. It is well-known that the reversibility in the doping of organic semiconductors is determined by the mass and charge transport in the electrolyte as well as by the electrical and structural properties of the polymer network. From the electrochemical results obtained under potentiodynamic control, CV-PANI-Prop films are strongly suggested to consist of a network characterized with pores of small size, likely in the nanoscale, but still easily permeable by solution species when compared to other thicker, denser, more compact, and hydrophobic polymers which exhibit lower reversibility in its doping/dedoping.

Further, our effort was focused in studying the potentiostatic electrosynthesis of PANI in this medium. To this end, PS-PANI-Prop films were grown onto GCE by chronocoulometry at a fix potential of +1.4 V (kept as high for comparison purposes). Figure 2 presents the post-preparation CVs registered for the films grown with several step durations (from 50 to 250 s, dashed lines). These were

compared with the last scan obtained for CV-PANI-Prop (dashed line). Step duration was kept intentionally low, to avoid significant degradation of the polymer by overoxidation of PB to side species. As expected, the profile exhibiting the best developed peaks was obtained upon application of the longest step (250 s). The figure inset reveals the existence of an obvious correlation between the step duration and the charge passed on the corresponding CV.

Curiously, peak currents for the film prepared with 250 s fell within the same order of magnitude with those for the CV-PANI-Prop prepared with 40 scans. Nevertheless, the changes observed in the shape of the CVs also suggest that the redox state and quality of the films are also affected by the synthetic procedure. For instance, a third oxidation peak was observed as a shoulder at +0.85 V. It could be argued whether it accounts for the activity of side species formed upon overoxidation of PB. However, no third reduction peak is observed when the potential was scanned back (unless it is overlapped with the second reduction peak at +0.55 V). Other differences involve: (a) the lower currents (and potential: +0.55 V) found for the oxidation of LB to ES, (b) the higher intensity, potential (+1 V), and splitting of the peak related with the oxidation of ES to PB, and (c) the higher currents found in the backwards process at +0.79 V.

Although deeper investigation is needed, these differences can be explained considering that PS-PANI-Prop presents an enhanced population for the ES form when compared with the CV-PANI-Prop. According to this view,
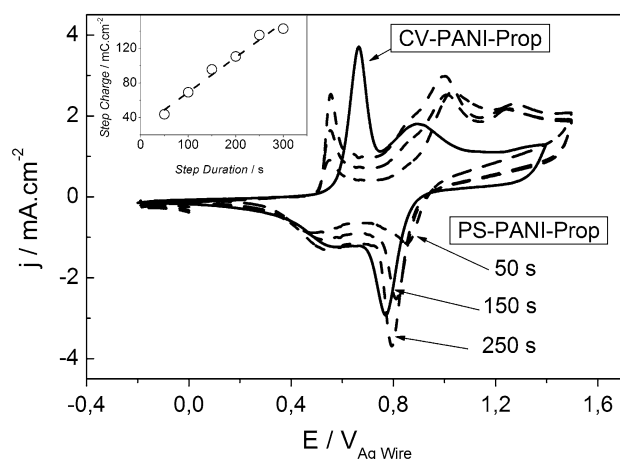
two types of ES forms will co-exist in the polymer during its doping, i.e., ES domains potentiostatically formed during the preparation process and those formed under their subsequent potentiodynamic doping. The splitting of the single peak corresponding to the oxidation of ES to PB in the CVs of PS-PANI-Prop could be due to the different energies associated with the oxidation of both types of ES forms.

Hence, it seems that the potentiostatic procedure yields better grown polymers simultaneously doped to deeper states which seems to affect the charge transport properties across the films as demonstrated by the establishment of doping/dedoping processes which are slightly more irreversible.

3.2 SEM

The morphology of both types of films was studied by ex-situ SEM. Images were acquired in secondary electron (SE) mode using an FEI Quanta 400 FEG/EDAX Genesis X4 M microscope at CEMUP (Centro de Materiais da Universidade do Porto). Figure 3 shows the micrographs taken for films grown by potentiodynamic (10 scans) and potentiostatic (100 s) methods (panels 3a and 3b, respectively) in the same conditions described above. Their comparison confirms that the potentiostatic approach drives to better grown PANI networks (characterized by a higher surface coverage and more compact structure) in shorter times than the potentiodynamic procedure.

Details on the structure and morphology of these networks are shown in the insets. CV-PANI-Prop films formed with such a low number of scans consisted of island-type deposits distributed onto a barely uncovered electrode surface. At this point, it is noteworthy that higher coverage can be simply achieved by increasing the number of scans (which was kept intentionally low for better comparison with the potentiostatic approach). These films presented a highly branched and crosslinked structure of PANI nanoribbons of about 100–80 nm width (and apparently lying parallel to the electrode surface) with pores around 150–250 nm. On the other hand, the potentiostatic method yielded a more homogenous and denser matrix of fibers, which appeared to be mostly vertically oriented, exhibiting a nanoparticulated morphology characterized by slightly larger pores and particle sizes. Agreeing with the electrochemical data, these results confirm that PANI films prepared by potential step are grown to a larger extent than those prepared by CV procedures of comparable duration.

3.3 UV–vis spectroscopy and conductivity measurements

Electrochromic properties and charge transport phenomena through these films were investigated by means of ex-situ spectroscopic measurements. UV–vis spectra were
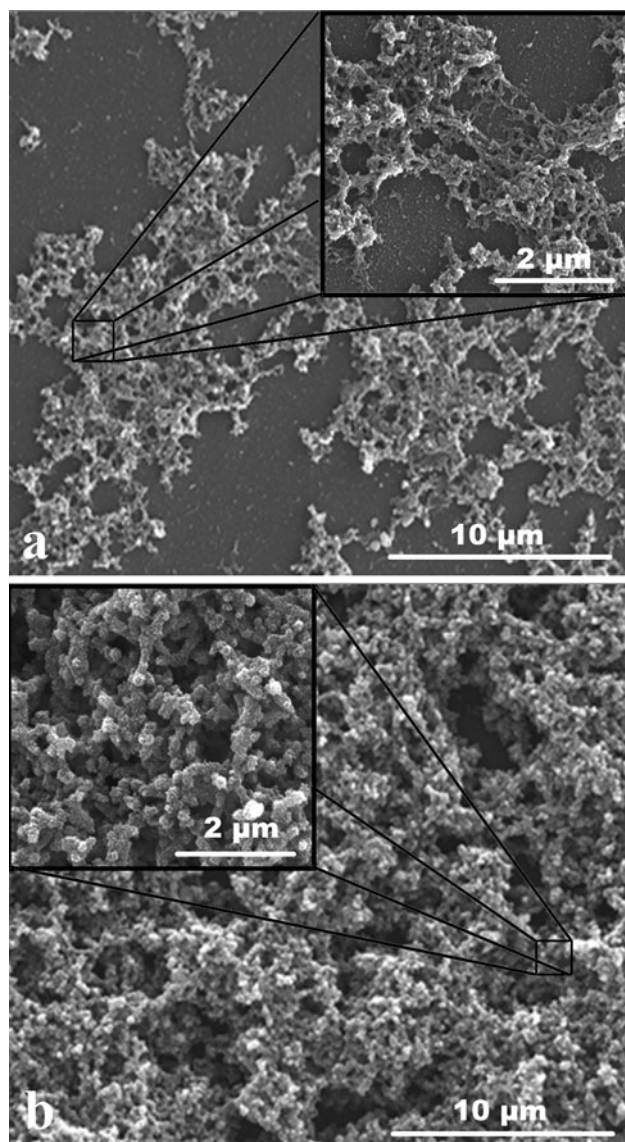

Fig. 2 CVs obtained after the electrosynthesis of PANI onto GCE from 0.7 M aniline + 1 M H_2SO_4 solutions in Propeline at 60 °C by potentiodynamic (CV-PANI-Prop) and potentiostatic procedures (PS-PANI-Prop). The *dashed lines* show the profiles for PS-PANI-Prop films prepared by the application of a potential step (from 0 to +1.4 V) of 50, 150, and 250 s duration. The profile of a CV-PANI-Prop film prepared with 10 scans between 0 and +1.4 V is shown for comparison purposes (*straight line*). The inset displays the charge density integrated under the step (*empty circles*) and the regression of the data to a straight line (*black dashed line*). The scan rate was 100 mV s^{-1} in all cases

Fig. 3 SEM pictures taken ex-situ in SE mode for GCE electrodes modified with CV-PANI-Prop (**a**) and PS-PANI-Prop films (**b**) prepared with 10 scans between 0 and +1.4 V and 100 s at +1.4 V, respectively. The accelerating voltage was 15 kV and the working distance (WD) ranged 8.5–10.8 mm in all cases. The *insets* represent an increase of the magnification factor from ×10,000–50,000

recorded on a Hitachi U-3000 spectrophotometer in the range 300–800 nm and using 1 cm path length quartz cuvettes. Optically transparent fluorine-doped tin oxide (FTO, Pilkington TEC 8, 6–9 Ω sq^{-1}, XopGlass, Castellón, Spain) glass sheets were cleaned by sequential immersion in ultrasonic baths of ethanol, acetone, and ultrapure water (about 15 min each). Later, they were used as working electrodes (immersed areas were measured with a precision caliper) in the electrochemical preparation of PANI. After preparation by different procedures, FTO/PANI substrates were placed into the cuvette (perpendicular to the light path) for the spectroscopic measurements.

To this end, PS-PANI-Prop films were electrosynthesized at +1.4 V for 100 s which was followed, or not, by another 200 s at 0 V. The UV–vis spectra registered for the films treated with, and without, such a dedoping step are shown in Figure 4 (dashed and straight curves, respectively) together with the chronoamperograms registered during their preparation (figure inset). The films which were not treated at 0 V were removed from the electrochemical cell at +1.4 V (as indicated in the figure). The spectrum obtained for a CV-PANI-Prop film prepared with 10 scans has also been included for comparison purposes (dotted curve). In the latter case, the simple eye inspection of the transparent substrates allowed us to witness reversible changes in film color, from pale yellow (0 V) to greenish-blue (+1.4 V), within each scan during its preparation. These changes can be taken as a first confirmation of the good electrochromic properties of CV-PANI-Prop.

The straight curve in Fig 4, agrees well with the typical spectrum of PANI in a doped form which consists of a peak at $\lambda = 440$ nm (A_{440}), a broad band in the range 500–800 nm ($A_{500-800}$, with a maximum near 700 nm), and a steep increase in the absorbance for $\lambda < 400$ nm (due to strong UV absorption of the glass substrate). The position of the first peak has been related to the protonation of the PANI-H_2O backbone, while the absorption band around 700 nm appears around 620 nm in the spectrum of the latter and is attributed to $n \to \pi^*$ electronic transitions [33–36]. This view was confirmed by the intense coloration (greenish-blue) exhibited by the film as it is shown in the picture inserts. As it is shown, the application of 200 s at
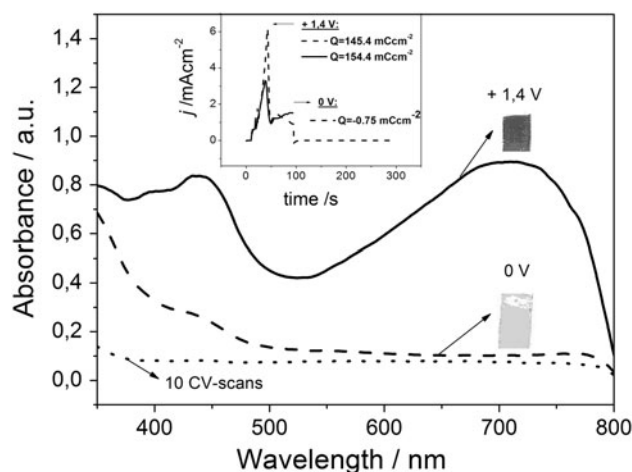

Fig. 4 Ex-situ UV–Vis spectra for a CV-PANI-Prop film prepared with 10 CV-scans at 100 mV s^{-1} and removed at 0 V (*dotted line*) and PS-PANI-Prop films grown by potential step to +1.4 V of 100 s followed (*dashed line*), or not (*straight line*), by 200 s at 0 V. Transparent FTO substrates were used in all cases. The insets present the amperometric transients (with the corresponding charges, Q, measured under them) and the pictures taken for the different PS-PANI-Prop films

0 V introduced drastic changes in the spectrum (partial and complete drop of A_{440} and $A_{500-800}$, respectively) and, thus, in the color of the film (pale yellow). Looking carefully to the chronoamperogram, it is strongly suggested that dedoping is extremely fast: i.e., 200 s is a time much longer than that necessary to achieve a nearly complete transition. The magnitude of the absorbance for the dotted curve was very low in the whole range of wavelengths investigated. Owing to the more limited conductivity of FTO, 10 scans may certainly lead to lower coverage than that observed in Figure 3a. But after all, it still seems possible to discriminate a profile similar to that exhibited by the dashed curve, just as expected from the reversible color changes witnessed during preparation. These results evidence that, both, CV-PANI-Prop and PS-PANI-Prop films, are able to undergo fast electrochromic transitions which is very interesting for certain applications in optoelectronic systems (smart windows, and so forth).

Fast charge transport processes in organic semiconductors require good organization in the layers and few defects, or charge traps, which may also be reflected in the electrical properties of these films. Accordingly, conductivity measurements were carried out by means of the standard four-probe technique using a custom fabricated cell. The conductivity (σ) of CV-PANI-Prop films prepared onto FTO substrate with 60 CV-scans and removed from solution at $+1$ V under a strong green coloration (typical of the conducting ES form) was measured (upon gentle removal of residual ionic liquid using a soft laboratory paper) following the Van de Pauw approach:

$$\sigma = (\ln 2/\pi d) \cdot (I/V) \tag{1}$$

where I is the current applied between 2 of these probes (0.1 A) and V is the voltage measured between the other couple of points (taken here as the average of 10 independent measurements). Film thickness (d) was determined to be around 10 μm from section images taken by SEM. The measured conductivity achieved a value of $\sigma = 56$ S cm^{-1} for the CV-PANI-Prop (60 scans). This value is around ten times higher that for PANI-H$_2$O synthesized by chemical or electrochemical means, which typically fall in the range between 2 and 6 S cm^{-1} [37, 38]. The chemical doping of PANI-H$_2$O has been reported to increase these values in one order of magnitude to $\sigma = 20$ S cm^{-1} [37].

Two types of intermolecular polymer chain conformations have been suggested to explain these differences: (a) a highly cross-linked *coil structure* characterized by enhanced inter-chain H-bonding network which introduces ring twisting and disrupts π-conjugation in the polymer backbone, thus, attenuating the conductivity [37], (b) a more *expanded coil structure* in which the H-bonding network is partially broken by the action of doping

molecules (such as m-cresol or THF) which strongly interact with the polymer. In the latter case, conductivity is increased owing to two types of effects: (a) conjugation defects are reduced as planarity between neighboring rings is enhanced; (b) a greater degree of polymer crystallinity is achieved. Conductivities in the range 35–50 S cm^{-1} have also been reported for PANI deposited onto a self-assembled monolayer terminated with certain transition metal complexes. The establishment of π type interactions between the π systems in the conjugated polymer and in the surface coordinated species were suggested to substantially stabilize an *expanded coil conformation* [39].

Thus, the use of Propeline as a preparation medium is demonstrated to induce a ten times increase in the conductivity of PANI with respect to that prepared in water. This result evidences the strong impact of the HBD species in the electrical properties of the polymer. The massive presence of choline and, specially, 1,2-ethanediol (a strong and bidentate H bond donor), may certainly disrupt the inter-chain H-bonding network, thus, favoring an *expanded coil structure* that explains the excellent conductivity found.

4 Conclusions

PANI films in the nanoscale can be easily prepared from mild Propeline electrolytes under potentiodynamic or potentiostatic procedures. The latter method has been shown to produce slightly better grown, more doped, and, potentially, more defective films when prepared during comparable times. Despite these differences, films with good quality have been obtained in both cases under the conditions investigated, as demonstrated by the good electroactivity, fast electrochromic transitions, and very high conductivities exhibited in all cases. Despite the fact that more work is needed to understand the correlation between DES properties and polymer performance (with the purpose of tailoring optical and electrical properties), in a general vein, the feasibility of the electrochemical synthesis of organic semiconductors since biodegradable and inexpensive ionic mixture has been demonstrated here. These results allow us to envision a future picture in which certain electropolymerization processes, currently performed from toxic organic solvents, can be adapted to be performed from the more environmentally friendly DES solvents.

References

1. Zein El Abedin S, Borissenko N, Endres F (2004) Electrochem Commun 6:422–426
2. Abbott AP, Capper G, McKenzie KJ, Ryder KS (2007) J Electroanal Chem 599:288–294
3. Sekiguchi K, Atobe M, Fuchigami T (2002) Electrochem Commun 4:881–885
4. Haerens K, Van Deuren S, Matthijs E, Van der Bruggen B (2010) Green Chem 12:2182–2188
5. Dyson PJ, Geldbach TJ (2007) Interface 16:50
6. Zhao D, Wu M, Kou Y, Min E (2002) Catal Today 74:157–189
7. Abbott AP, Dalrymple I, Endres F, MacFarlane DR (2008) In: Endres F, MacFarlane D, Abbott A (eds) Electrodeposition from Ionic Liquids. WILEY-VCH Verlag GmbH & Co., KGaA, Weinheim
8. Abbott AP, Griffith J, Nandhra S, O'Connor C, Postlethwaite S, Ryder KS, Smith EL (2008) Surf Coat Technol 202:2033–2039
9. Shahbaz K, Mjalli FS, Hashim MA, AlNashef IM (2011) Thermochim Acta 515:67–72
10. Abbott AP, El Ttaib K, Ryder KS, Smith EL (2006) Electrochim Acta 51:4420
11. Jhong H, Wonga D, Wana C, Wang Y, Wei T (2009) Electrochem Commun 11:209
12. Abbott A, Cullis P, Gibson M, Harris R, Raven E (2007) Green Chem 9:868
13. Jain N, Kumar A, Chauhan S (2005) Tetrahedron 61:1015
14. Tripathi BP, Shahi VK (2011) Prog Polym Sci 36(7):945–979
15. Snook GA, Best AS (2009) J Mater Chem 19:4248–4254
16. Lange U, Roznyatovskaya NV, Mirsky VM (2008) Anal Chim Acta 614:1–26
17. Malinauskas A (1999) Synth Met 107:75–83
18. Illing G, Hellgardt K, Schonert M, Wakeman RJ, Jungbauer A (2005) J Membr Sci 253:199–208
19. Bessière A, Duhamel C, Badot J-C, Lucas V, Certiat M-C (2004) Electrochim Acta 49:2051–2055
20. Gorke JT, Srienc F, Kazlauskas RJ (2008) Chem Commun 2008:1235–1237
21. West RJ, Davis JW, Pottenger LH, Banton MI, Graham C (2007) Environ Toxicol Chem 26:862–871
22. Costa R, Figueiredo M, Pereira CM, Silva F (2010) Electrochim Acta 55:8916–8920
23. Bazito FFC, Silveira LT, Torresia RM, Cordoba de Torresi SI (2008) Phys Chem Chem Phys 10:1457–1462
24. Dalmolin C, Canobre SC, Biaggio SR, Rocha-Filho RC, Bocchi N (2005) J Electroanal Chem 578:9–15
25. Watanabe A, Mori K, Iwasaki Y, Nakamura Y (1987) Macromolecules 20:1793–1797
26. Pekmez N, Pekmez K, Yildiz A (1994) J Electroanal Chem 370:223
27. Dinha HN, Birss VI (2000) J Electrochem Soc 147:3775
28. Chen W-C, Wen T-C, Gopalan A (2005) Synth Met 128:179
29. Cao Y, Smith P, Heeger AJ (1992) Synth Met 48:91
30. Pang Y, Xu H, Li X, Ding H, Cheng Y, Shi G, Jin L (2006) Electrochem Commun 8:1757–1763
31. Lana-Villarreal T, Campiña JM, Guijarro N, Gómez R (2011) Phys Chem Chem Phys 13:4013–4020
32. Li MC, An Ma C, Liu BY, Jin ZM (2005) Electrochem Commun 7:209–212
33. Stejskal J, Sapurina I, Prokeš J, Zemek J (1999) Synth Met 105:195–202
34. Somani PR, Radhakrishnan S (2002) Mater Chem Phys 77:117–133
35. Taleghani HG, Aleahmad M, Eisazadeh H (2012) Synth Met 161:2638–2640
36. Tetsuo H, Takumi N, Noriyuki K (2006) Synth Met 156:1327–1332
37. Zheng W, Min Y, MacDiarmid AG, Angelopoulos M, Liao Y-H, Epstein AJ (1997) Synth Met 84:63–64
38. Qin Q, Tao J, Yang Y (2010) Synth Met 160:1167–1172
39. Sarno DM, Martin JJ, Hira SM, Timpson CJ, Gaffney JP, Jones WE Jr (2007) Langmuir 23:879–884